

Figure 5: Variance convergence speed on SVHN. x-axis: epochs, y-axis: $\ln \sigma$. We see that the shared σ -VAE which optimizes the variance with gradient descent has an initial period of convergence when the variance converges to the region of the optimal value. In contrast, σ -VAE with analytical (optimal) variance quickly learns a good estimate of the variance, which leads to better performance. The unit variance Gaussian β -VAE can be interpreted as having a constant variance determined by β , shown here. Since the variance doesn't change throughout training, it achieves suboptimal performance.

450 A Additional experimental results

451 In this section, we provide more qualitative results as well as a graph showing the convergence
 452 properties of the variance for different models.

453 B Experimental details

454 For the image VAE models, the en-
 455 coder has 3 convolutional layers fol-
 456 lowed by a fully connected layer,
 457 while the decoder has a fully con-
 458 nected layer followed by 3 convolu-
 459 tional layers. The β was tuned from
 460 100 to 0.0001 for β -VAE. The number
 461 of channels in the convolutional layers
 462 starts with 32 and increases 2 times in
 463 every layer, except on the CIFAR data,
 464 where it starts with 128. The dimen-
 465 sion of the latent variable is 20. Adam
 466 [24] with learning rate $1e-3$ is used
 467 for optimization. Batch size of 128
 468 was used and all models were trained
 469 for 10 epochs. Unit Gaussian prior
 470 and Gaussian posteriors with diagonal
 471 covariance were used. For the SVG
 472 models, the original hyperparameters for the SVG-LP model were used. We use the standard
 473 train-val-test split for all datasets. All models were trained on a single high-end GPU.

Table 4: ELBO on discretized data. All distributions except categorical have scalar scale parameters. The σ -VAE performs well on the discretized ELBO metric, performing similarly to a discrete distribution parametrized as a discretized Gaussian or discretized Logistic. Full categorical distribution attains highest likelihood due to having the most statistical power.

	CIFAR VAE		
	$-\log \text{pdf} \downarrow$	$-\log p \downarrow$	FID \downarrow
Categorical VAE		< 10673	137.6
Gaussian VAE	< 740.5	< 15131	212.7
Gaussian σ -VAE	< -896.1	< 11120	136.7
Disc. Gaussian σ -VAE		< 11117	136.9
Disc. Logistic σ -VAE		< 11103	136.7



Figure 6: Samples from the σ -VAE (left) and the Gaussian VAE (right) on the SVHN dataset. The Gaussian VAE produces blurry results with muted colors, while the σ -VAE is able to produce accurate images of digits.

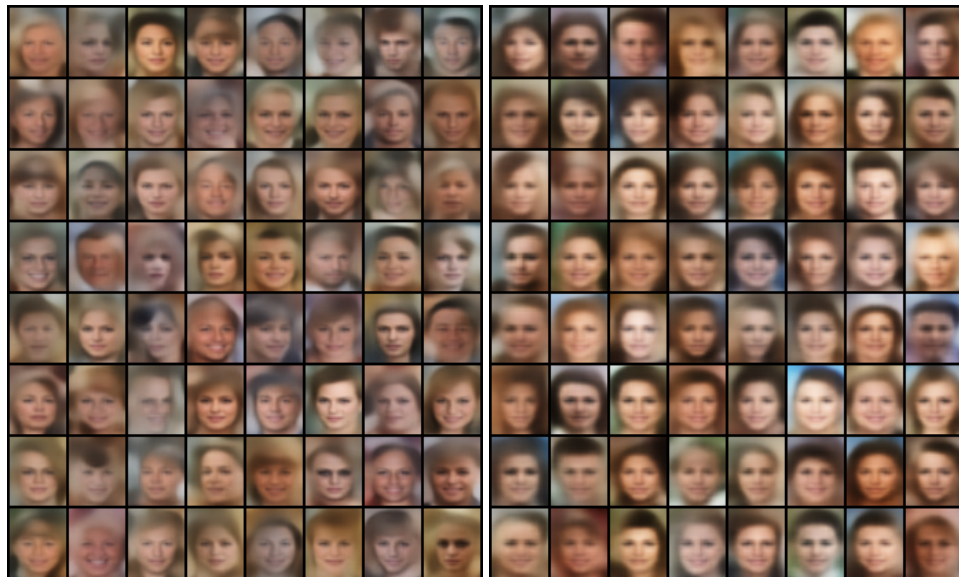


Figure 7: Samples from the σ -VAE (left) and the Gaussian VAE (right) on the CelebA dataset, images cropped to the face for clarity. The Gaussian VAE produces blurry results with indistinct face features, while the σ -VAE is able to produce accurate images of faces.

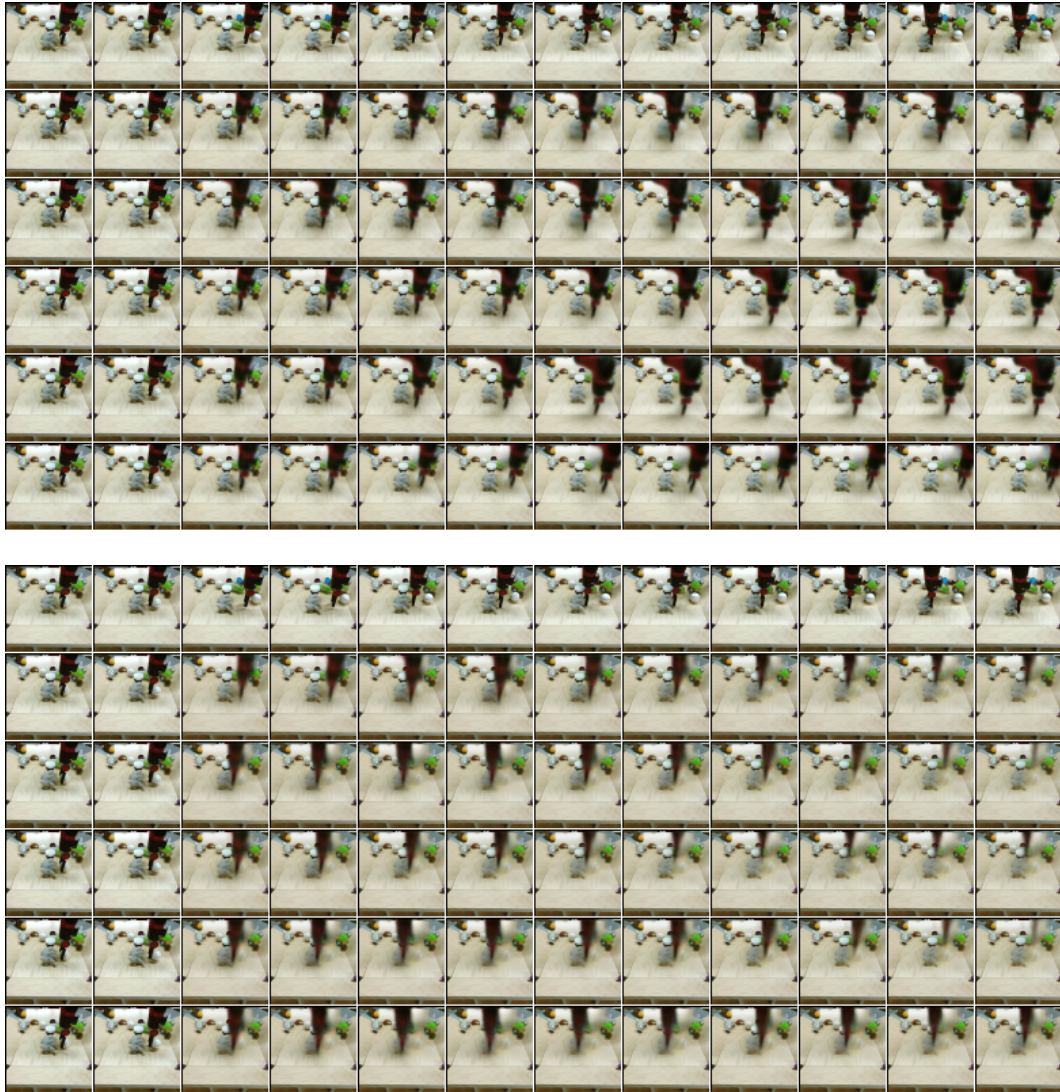


Figure 8: Samples from the σ -VAE (top) and the Gaussian VAE (bottom) on the BAIR dataset. Sampled sequences conditioned on two initial frames are shown, and the ground truth sequence is shown at the top. The Gaussian VAE produces blurry robot arm texture and the arm often disappears towards the end of the sequence, while the σ -VAE is able to produce sequences with realistic motion and model the details of the arm texture, such as the gripper.



Figure 9: Samples from the σ -VAE (left) and the Gaussian VAE (right) on the challenging CIFAR dataset. The Gaussian VAE produces blurry results with muted colors, while the σ -VAE models the distribution of shapes and colors in the CIFAR data more faithfully.

474 C Alternative Decoder Choices

475 We describe the alternative decoders evaluated in Table 2: using the Beta, the bitwise-categorical,
 476 and the logistic mixture distributions.

477 **Beta VAE** Previously described continuous distributions such as Gaussian had positive density on
 478 the whole real line, $(-\infty, \infty)$. This might be undesirable since pixel intensity values lie in a finite
 479 range, usually scaled to $[0, 1]$. These continuous distributions therefore assign positive densities to
 480 impossible intensity values, potentially leading to poor likelihood and invalid samples. We therefore
 481 evaluate a continuous distribution that is defined on the $[0, 1]$ range, specifically, the Beta distribution.
 482 We parametrize the Beta distribution with the two concentration parameters produced per pixel and
 483 channel. We experimented with alternative location-scale parametrizations, however, we found that
 484 the parametrization via concentration parameters allows to enforce that the distribution is defined on
 485 the inclusive interval $[0, 1]$, by restricting both concentration parameters to be higher than 1. This is
 486 harder to enforce with location-scale parametrizations. In our experiments, we found that the Beta
 487 distribution does not outperform the σ -VAE decoder, as the Gaussian σ -VAE decoder can ensure
 488 that the values outside of the $[0, 1]$ range have small density values by setting the variance to be
 489 small. However, we expect the Beta distribution to be useful for enforcing that the model only assigns
 490 positive densities to values in a certain range.

491 **Bitwise-categorical VAE** While the 256-way categorical decoder described in Section 3.2 is
 492 very powerful due to the ability to specify any possible intensity distribution, it suffers from high
 493 computational and memory requirements. Because 256 values need to be kept for each pixel and
 494 channel, simply keeping this distribution in memory for one 3-channel 1024×1024 image would
 495 require 3 GiB of memory, compared to 0.012 GiB for the Gaussian decoder. Therefore, training deep
 496 neural networks with this full categorical distribution is impractical for high-resolution images or
 497 videos. The bitwise-categorical VAE improves the memory complexity by defining the distribution
 498 over 256 values in a more compact way. Specifically, it defines a binary distribution over each bit in
 499 the pixel intensity value, requiring 8 values in total, one for each bit. This distribution can be thought
 500 of as a classifier that predicts the value of each bit in the image separately. In our implementation
 501 of the bitwise-categorical likelihood, we convert the image channels to binary format and use the
 502 standard binary cross-entropy loss (which reduces to binary log-likelihood since all bits in the image
 503 are deterministically either zero or one). While in our experiments the bitwise-categorical distribution
 504 did not outperform other choices, it often performs on par with our proposed method. We expect
 505 this distribution to be useful due to its generality as it is able to represent values stored in any digital
 506 format by converting them into binary.

507 **Logistic mixture VAE** For this decoder, we adapt the discretized logistic mixture from Salimans
508 et al. [44]. To define a discrete 256-way distribution, it divides the corresponding continuous
509 distribution into 256 bins, where the probability mass is defined as the integral of the PDF over
510 the corresponding bin. [26] uses the logistic distribution discretized in this manner for the decoder.
511 Salimans et al. [44] suggests to make all bins except the first and the last be of equal size, whereas
512 the first and the last bin include, respectively, the intervals $(-\infty, 0]$ and $[1, \infty)$. Salimans et al. [44]
513 further suggests using a mixture of discretized logistics for improved capacity. Our implementation
514 largely follows the one in Salimans et al. [44], however, we note that the original implementation is
515 not suitable for learning latent variable models, as it generates the channels autoregressively. This will
516 cause the latent variable to lose color information since it can be represented by the autoregressive
517 decoder. We therefore adapt the mixture of discretized logistics to the pure latent variable setup
518 by removing the mean-adjusting coefficients from [44]. In our experiments, the logistic mixture
519 outperformed other discrete distributions.